ISSN 1590-8844
International Journal of Mechanics and Control, Vol. 16, No. 01, 2015

SIMULATION AND CONSTRUCTION OF A MEMS CSFH BASED MICROGRIPPER

Nicola P. Belfiore* Giovanni B. Broggiato* Matteo Verotti* Marco Balucani** Rocco Crescenzi** Alvise Bagolini*** Pierluigi Bellutti*** Maurizio Boscardin***

* Department of Mechanical and Aerospace Engineering, Sapienza University of Rome, Italy

** Department of Information Engineering, Electronic and Telecommunications, Sapienza University of Rome, Italy

*** Fondazione Bruno Kessler (FBK), Micro Nano Facility (MNF), Italy

ABSTRACT

This paper describes the design, simulation, construction process and experimental analysis of a microgripper, which makes use of a new concept hinge, called CSFH (Conjugate Surfaces Flexure Hinge). The new hinge combines a curved cantilever beam, as flexible element, and a pair of conjugate surfaces, whose contacts depend on load conditions. CSFHs improve accuracy and guarantee that minimum stress conditions hold within the flexible beam. This microgripper is designed for Deep Reactive-Ion Etching (DRIE) construction process and comb-drive actuation. Theoretical basis and Finite Element Analysis (FEA) simulations have been employed in order to predict the feasibility of the device under construction. Finally, some experimental evidence of the construction process has been provided.

Keywords: Microgripper, MEMS, Conjugate surfaces flexure hinge, DRIE

1 INTRODUCTION

Micro-grippers have been increasingly employed in many applications during the last decades thanks to the continuous improvements in MEMS-based Technologies.

In 1995, a piezoelectric milligripper [1] for in vivo tissue manipulation has been optimized in order to obtain a maximum gripping force. In the same paper, a cochlear electrode implant has been suggested, also, in order to stimulate the auditory nerve and, so, restore hearing to the profoundly deaf. Then, a micro needle has been proposed for skin painlessly puncturing and drugs delivery. Finally, a microbiological assay device has been presented to quantify yeast cells metabolic growth rate. In the same year, multicomponent force-displacement sensing techniques, which are particularly useful at the micro scale, have been discussed [2].

Contact author: Nicola P. Belfiore[1]

[1] Dept. Mechanical and Aerospace Engineering, Sapienza University of Rome. Via Eudossiana 18, 00184 Rome, Italy.
E-mail: belfiore@dima.uniroma1.it

In 2001, specially designed micro-grippers [3] with force-feedback have been presented for the handling of pieces with sizes from 10 μm up to 2 mm. The mechanisms have been built by using wire electro-discharge-machining of spring steel. In 2002, SU-8 photoepoxy [4] has been adopted in order to build micro valves and micro-grippers with good aspect ratio, equipped with beams and hinges with in-plane compliance. In the same work, the elastic properties of the material has been measured by employing a tactile force sensor.

In 2004, a transparent electrostatic gripper [5] has been used to build a miniature assembly cell for MEMS assembly and packaging. Thanks to the gripping force and stage positioning accuracy, insertion operation of 500 μm wide parts in 550 μm wide slots etched in silicon wafers were possible. In 2006, a multi-objective optimization [6] has been suggested in order to improve the design of micro-grippers by taking into account performance metrics and design constraints. Lumped spring and pseudo-rigid-body model approximations have been used in the optimization process. In 2007, out-of-plane piezoelectric micro-grippers have been presented [7]. Thanks to the electromechanical and gripping characteristics and to micro cantilevers actuation, these gripper accurately handled 100 μm diameter metallic ball without any adhesion problems between two jaws of gripper and the ball. In 2008, a precision manipulator and a micro gripper have been presented for micro assembling [8]. The PRR 3 DoF manipulator, which has been actuated by modular revolute and prismatic actuators, was equipped with a micro-gripper MEMS-Technology based end-effector, whose jaws displacement was up to about 143 μm. A real gripping test has been also conducted to evaluate the robotic system. In the same year, a MEMS based piezoresistive sensor has been designed, for micro-force measurement and a resolution within the micronewton range could be achieved, by means of surface and bulk micromachining technology on single crystal silicon wafer [9]. Boron diffusion process, combined with Deep Reactive Ionic Etching (DRIE), has been used to form side direction force sensors. In 2009, a four arms structure MEMS gripper integrated sidewall piezoresistive force sensor has been designed [10,11]. Vertical sidewall surface piezoresistor etching technique has been used to form the side direction force sensors. An electrostatically driven microactuator has been also designed to provide the force to operate the other two movable arms. In the same year, a versatile MEMS gripper has been designed and fabricated, with the MetalMUMPs process, for two-dimensional manipulation [12]. This has been accomplished by a multiple DoF electrothermal actuator which can achieve independent in-plane and out-of-plane motions. A novel electro-thermal 100 μm device layer micro-gripper has been presented also in Ref. [13], where 1-D steady state heat equations have been used in order to model the thermal behaviour of a general 5 lineshape microbeam's actuator. Another MEMS micro-gripper [14] has been integrated with a plunging mechanism in order to impact the micro object and gain sufficient momentum to overcome adhesion forces. This device was able to achieve 100 % successful release rate on 200 trials, with an accuracy of 0.70±0.46 μm in the the manipulation of 7.5 − 10.9 μm borosilicate glass spheres under an optical microscope. In 2010, a three DoF meso/micromanipulation system has been developed and tested for handling microobjects [15], for example, biological cells and microbeads.

In the same year, Havlik suggested a method for minimizing compliance errors and a calibration procedure for multi DoF positioning or multi-component sensing devices based on compliant mechanisms [16]. Furthermore, some design problems of compliant mechanisms for particular devices were discussed and an optimization procedure was applied for designing compliant joints [17]. In 2011, an electrothermally driven MEMS gripper has been designed, fabricated and characterized [18, 19]. The system uses a new metallic V-shape actuator and a set of modified Guckel U-shape actuators. In 2012, a new MEMS-Technology based micro-gripper has been developed to serve as micromanipulation robotic system [20]. The *pseudo-rigid body mechanism* has been used to model the manipulator and to estimate the grip force. Results have been verified by simulations and experiments. In the same year, a novel monolithic nano-micro-gripper structure has been simulated (motion and control) for biologic cells manipulation [21]. In 2013, an electrostatic comb-drives actuated MEMS micro-gripper, with an integrated electrothermal force sensors, has been presented for biomedical and micro industrial applications [22, 23]. This structure has been fabricated in a Silicon On Insulator (SOI) MEMS foundry (MEMSCAP).

In 2014, an electrothermal actuator with two DoF and independent in-plane and out-of-plane motions has been presented [24]. The structure has been fabricated with the Metal MUMPs, which offers silicon nitride, polysilicon, and nickel as the major structural materials. Thanks to this method, new micro-grippers with 2-D manipulation can be constructed with two actuators, each of which serves as the gripper arm. Another micro-gripper with two grade displacement amplification has been designed, simulated and fabricated, based on flexible hinges, and actuated by piezoelectric ceramics [25].

The Authors of the present investigation have been also involved in the development of grippers and micro-grippers and MEMS-Technology based devices.

In 1997, an atlas of 64 linkage-type grippers has been presented [26]. For each mechanism, the graph representation and one of the possible functional schematic have been provided. The adopted enumeration methodology has been based on Graph Theory and an extension of the concept of isomorphism to the class of actuated mechanisms has been recalled. In 2000, some issues related to some peculiar characteristics of plane kinematic chains have been introduced [27, 28], while some years later some problems related to the tribological behaviour of mechanical components have been analyzed [29–31]. In 2010, the development of a 3 DoF plane micro platform with remote system of actuation has been presented [32]. MEMS Technology has been used to develop this system which has been built and simulated through FEA. The whole device overall size was less than 4mm. In 2011, a new multibody system code, based on Lagrange Multiplier method of dynamic analysis, has been applied to the *pseudo-rigid body model* of a micro-compliant mechanisms for studying the static and dynamic analysis [33]. In 2012, the performance of compliant parallel micromanipulators [34] has been evaluated in terms of the *MA*, mechanical advantage, and *k(J)*, kinematic condition number (see also Refs. [35–37] for index characterization). This evaluation has been done on the pseudo-rigid body equivalent mechanism, by means of a new and fast method for direct kinematic analysis of parallel manipulators. In 2013, a plane parallel micromanipulator has been presented for general purposes in-plane micropositioning and a numerical procedure has been used in order to optimize some kinetostatic performance indices [38]. The approach has been based on a refined simplification of the direct kinematic problem and it is applied to the pseudo-rigid body equivalent model of the original compliant mechanism. Genetic Algorithms have been used for the global optimization of these parameters.

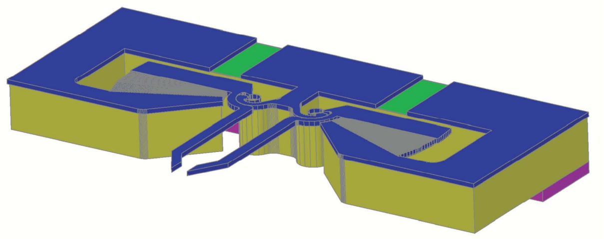

Figure 1 Pictorial view of the gripper as it was mounted on the chip.

Finally, an early version of a MEMS-Technology based micro-gripper, which is based on a new flexural hinge, has been designed for cell manipulation after FEA-assisted simulations and improvements [39].
At the beginning of 2014, a new method of functional synthesis of a new class of MEMS has been disclosed [40]. The design approach is based on CSFHs and on the accurate detection of the pseudo-rigid-body equivalent mechanism, which allows the application of several classic algorithms well known in kinematic synthesis (see for example Ref. [41, 42]). In the same year, the Authors made an attempt to offer a contribution to the experimental analysis of tribological issues in MEMS [43] and, so, a new concept design of a microtribometer for testing silicon-silicon sliding in-MEMS devices has been presented. A dedicated MEMS has been designed, whose only purpose is recreating silicon-silicon sliding under prescribed loads and, then, assessing friction and wear.
In the present paper, a new comb-driven actuated silicon micro-gripper, depicted in Fig. 1, will be presented and in the following paragraphs its design, physical construction, and experimental analysis will be discussed.

2 GRIPPER DESIGN AND SIMULATION

The adopted design method is based mainly on the choice of embedding so-called CSFHs, Conjugate Surfaces Flexure Hinges [44], within the gripper layout. The main advantage of adopting this kind of hinges consists in the possibility of being manufactured by means of planar technology processes. Although the CSFH hinge can be built at any scale, the new component is believed to give its best at the microscale, where most of MEMS-Technology based processes perform successfully on silicon wafers. The CSFH is composed of two main parts: *a)* a flexible curved beam and *b)* a portion of revolute joint conjugate surfaces. Fig. 2 shows one of the possible configurations for a CSFH. The two bodies $\mathcal{A}$ and $\mathcal{B}$ are joined by means of a thin curved beam, which, on the action of external torques and forces, deflects much more than the pseudo-rigid bodies $\mathcal{A}$ and $\mathcal{B}$, whose thickness makes their deformation negligible with respect to the curved beam deflection On the other hand, bodies $\mathcal{A}$ and $\mathcal{B}$ make up a kinematic pair with circular conjugate profiles, as the Figure displays, which are the so-called kinematic elements of the pair $\mathcal{A}$ and $\mathcal{B}$.

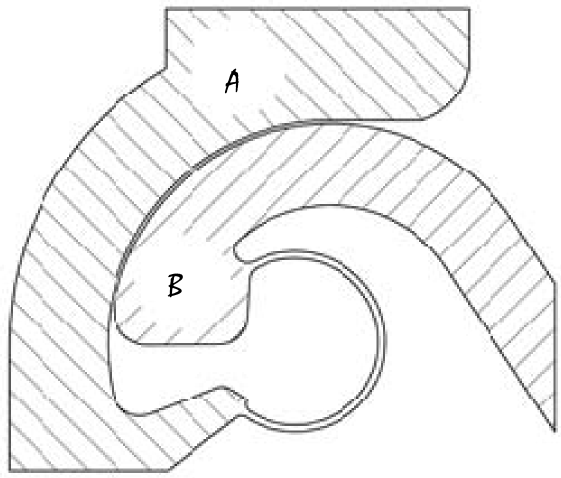

Figure 2 Schematic representation of the CSFH hinge connecting parts $\mathcal{A}$ and $\mathcal{B}$.

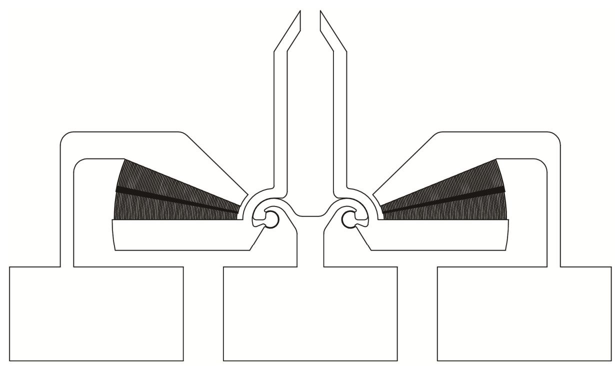

Figure 3 Front view of the gripper device.

According to the original idea [45], the curved beam elastic weights center is positioned in correspondence of the center of the conjugate profiles.

2.1 DESIGN

Since MEMS-Technology based silicon devices are, essentially, compliant mechanisms the method based on the pseudo-rigid body equivalent mechanism can be adopted [46–48]. However, the gripper presented in this paper has two hinges only, and so the kinematic structure is rather elementary. In fact, the pseudo-rigid equivalent mechanism consists in two links connected, independently, to the frame link. Fig. 3 shows how the two claws are allowed to rotate about rotation centers which keep stationary during motion. Although the topological structure is very simple for the proposed case, its actual design and dimensioning is not trivial at all. For this reason it is necessary to use both theoretical and numerical tools in order to predict the forces and torques and to simulate the gripper motion during operation. A theoretical approach for simulation of CSFH-equipped compliant mechanisms has been recently suggested [49].

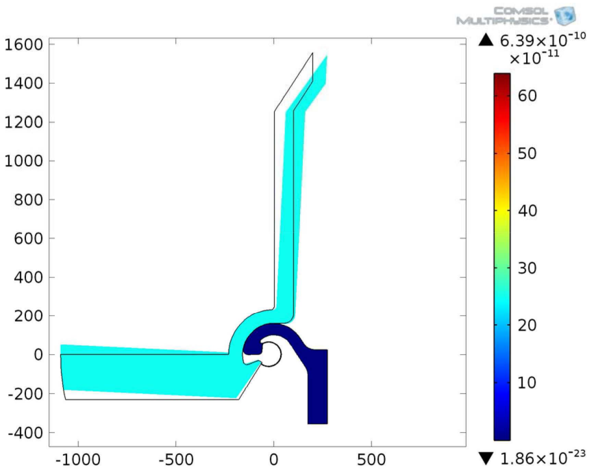

Figure 4 Results of preliminary simulation: single jaw.

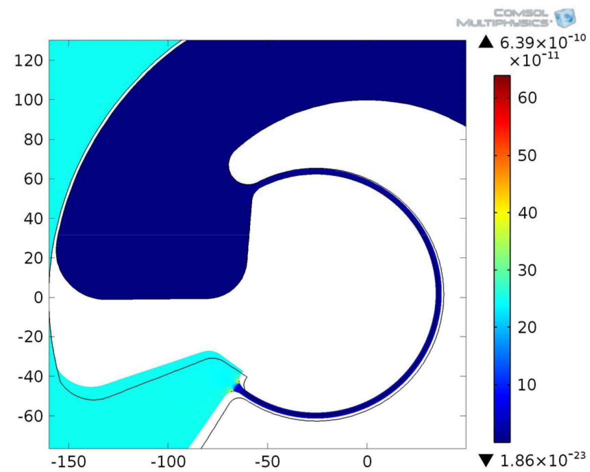

Figure 5 Results of preliminary simulation: curved beam.

This method has been proposed for the inverse kinetostatic analysis of compliant four-bar linkages with flexible circular joints and pseudo-rigid bodies. The theory of curved beams has been applied to the flexible parts and a novel closed form symbolic expression has been presented for the compliance matrix, which maps the generalized forces and relative displacements for the free section of the curved beam with respect to the framed one. The theory of planar displacement matrices has been applied in order to solve the static balance of the whole system. The method has been applied at the microscale.
The following paragraph will describe how Finite Element Analysis can be used in order to simulate the gripper under development.

2.2 PRELIMINARY SIMULATION

A preliminary simulation was performed in Comsol Multiphysics, by imposing a prescribed rotation of the movable comb drive with respect to the center of the conjugate surfaces. In first approximation, an isotropic material was considered (with E = 160 GPa and μ = 0.28), and a rotation angle equal to 2.75 ∘. Figures 4 and 5 show the whole simplified gripper and the flexure hinge, respectively.

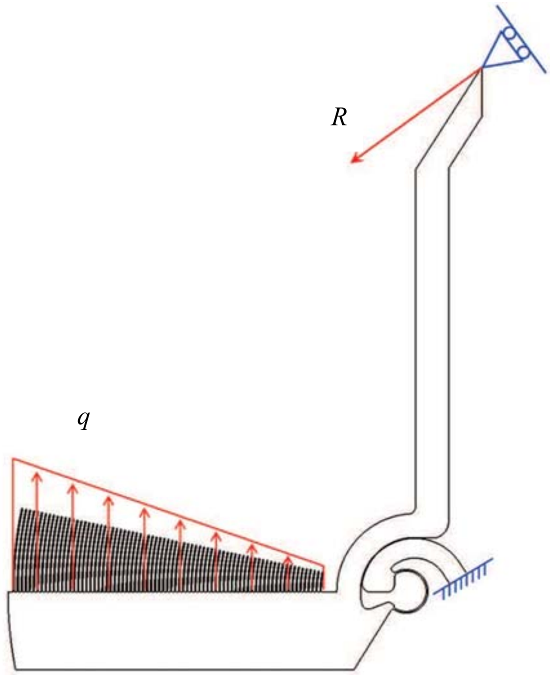

Figure 6: Static simulation under the action of a reaction force *R* and a linearly distributed load *q*

2.3 MICRO-GRIPPER STRUCTURAL MODEL

In order to study the micro-gripper mechanical behaviour a Finite Element model has been built. It takes into account a single grip jaw loaded on the comb drive arm by distributed load and constrained on the gripper tip to tighten flat or cuneiform bodies which react with differently oriented forces (see Fig. 6).
The aim of the analysis has been to evaluate the movements of the hinge centre and of the actuator fingers to identify the load conditions that imply the closure of gap between hinge conjugate surfaces or that involve the risk of contact between the two combs. Besides, in all the studied load conditions, the stress state of curved beam has been monitored to detect possible critical loads and to get hints for a future topological optimization.
Two-dimensional plane-strain elements have been used to model the flexural beam and the gripper jaw. Figures 7 and 8 show the mesh details (the CSFH and the flexible beam, respectively) generated with the commercial software ANSYS. All the analyses have been run by large displacement solver, simulating both the phase when the jaws approach each other (where the comb-drive works just

against the beam elastic reaction) and the phase when their clenching against a rigid body that has been modelled as a roller constraint. In addition, the roller sliding plane has been oriented from zero to 75° to generate an oblique reaction force on the gripper tip, as already mentioned.

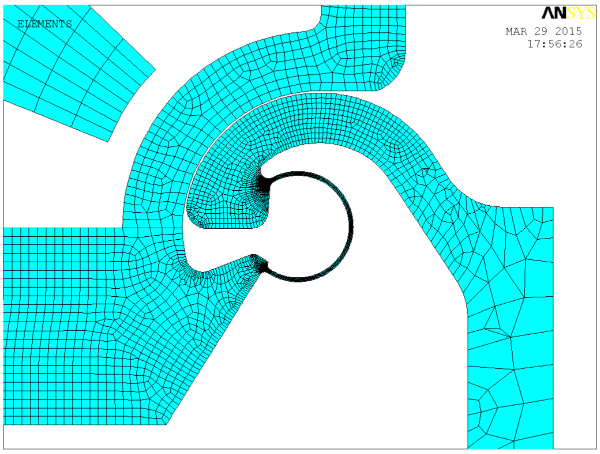

Figure 7 Finite-element mesh: CSFH.

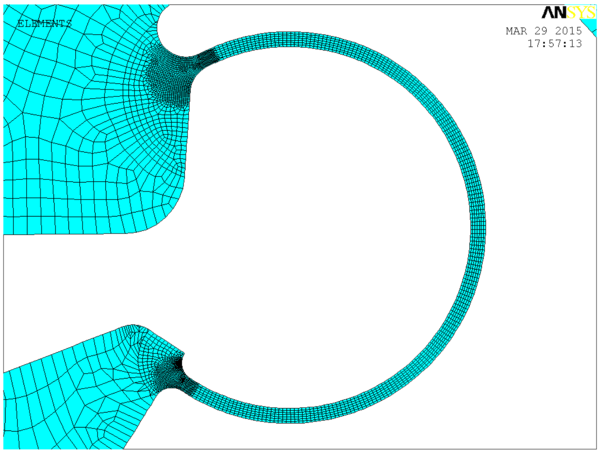

Figure 8 Finite-element mesh: flexible beam.

The comb-drive has been actuated applying a linear variable negative pressure on the mobile arm up to reach a torque moment equal to 0.6 μNm.

The diagrams shown in Fig. 9 confirm that, during free closure, the jaw motion is a pure rotation around hinge centre. In fact, when the complete closure is reached, for

- gripper tip travel: 75 μm,
- jaw rotation: 2.75°,
- applied torque: 0.0125 μNm and
- estimated actuation voltage: 40 V,

the off-centre displacement is less that 0.015 μm along X direction, and about 0.065 μm along Y direction (Y component of displacement is larger because of off axis action of comb force). Also, during this phase, finger gap deviation from initial value is at most 0.004 μm.

Critical tightening condition may be identified looking at Fig. 10, where the minimum gap between hinge conjugate surfaces and between comb fingers are plotted as a function of applied torque. It can be noticed that only hinge gap depends on reaction force direction, and that quite high external load are required to cause hinge gap closure.

Instead, independently from tip reaction orientation, excessive actuation torque (larger than 0.45 μNm) may cause dangerous contacts among comb fingers.

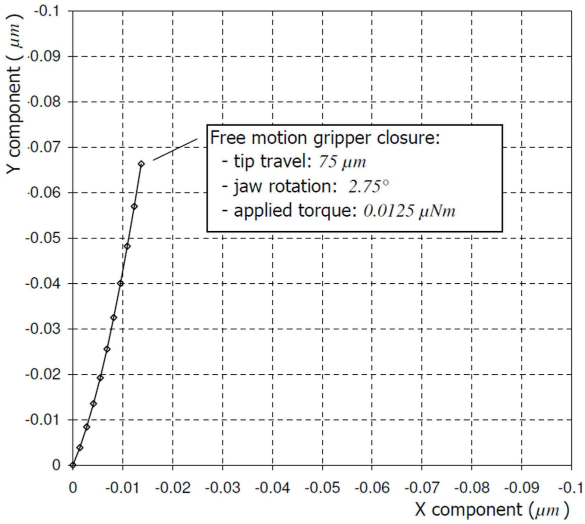

Figure 9 Off-center displacements along X and Y axes.

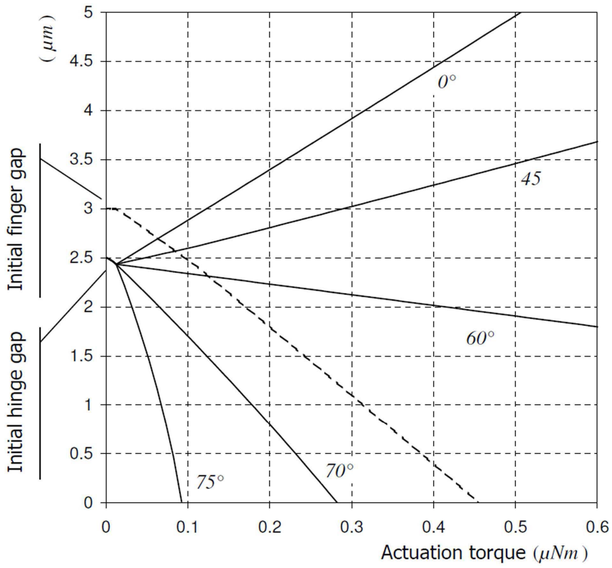

Figure 10 Finger contact avoidance design chart, for different directions of R.

3 COMB DRIVES ANALYSIS

With reference to Fig. 11, the capacitance associated to each comb finger is composed of two terms, one resulting from the finger gaps, g, and one resulting from the distance between the finger free-end section and the side wall surface of the opposite comb system, depending on the angle a. In most practical cases, the latter is sufficiently small to be neglected [50].

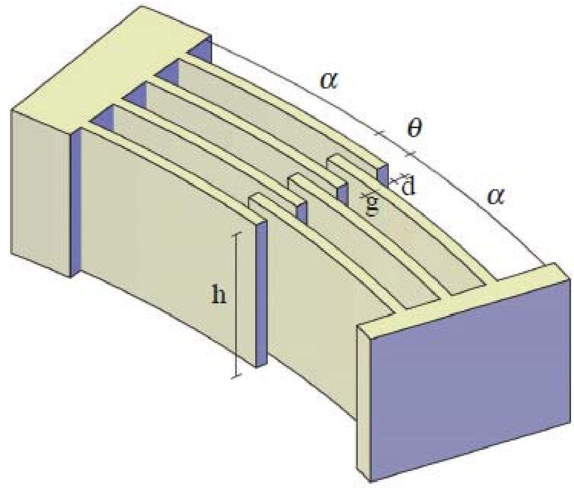

Figure 11 Comb-drive actuator geometric parameters.

Table I - Geometric parameters of the comb drive actuator

Geometric parameter	model 1	model 2
Thickness of the device layer (h)	40 μm	40 μm
Finger width (d)	3 μm	2 μm
Finger gap (g)	3 μm	2 μm
Number of fingers	77	100
Finger angle (α+θ)	12°	12°
Finger initial overlap (θ)	2°	2°

The total capacitance C_T can then be calculated as [51]:

$$C_T = \varepsilon_0 h\theta \left[\sum_{i=1}^{n-1} (\ln A)^{-1} + \sum_{i=0}^{n-1} (\ln B)^{-1} \right], \quad (1)$$

where

$$A = \frac{r_0 + 2i(d+g)}{r_0 + 2i(d+g) - g},$$

$$B = \frac{r_0 + (2i+1)(d+g)}{r_0 + 2i(d+g) + d}.$$

In the previous equation, ε_0 is the vacuum permittivity, h is the thickness of the device layer, θ is the overlap angle, n is the number of fingers in the comb, r_0 is the radius of the first finger, and d is the finger width.
The corresponding electrostatic torque can be determined by [50]:

$$\tau = \frac{1}{2}\left(\frac{\partial C_T}{\partial \theta}\right) V^2, \quad (2)$$

where V is the applied voltage. Substituting (1) in (2), we obtain

$$\tau = \frac{1}{2}\varepsilon_0 h V^2 \left[\sum_{i=1}^{n-1} (\ln A)^{-1} + \sum_{i=0}^{n-1} (\ln B)^{-1} \right]. \quad (3)$$

In the present investigation, two different models are considered, characterized by different finger width, gap, and total number. Table 1 lists the values of the geometric parameters for each model. The torque values for different applied voltage values are shown in Fig. 12.

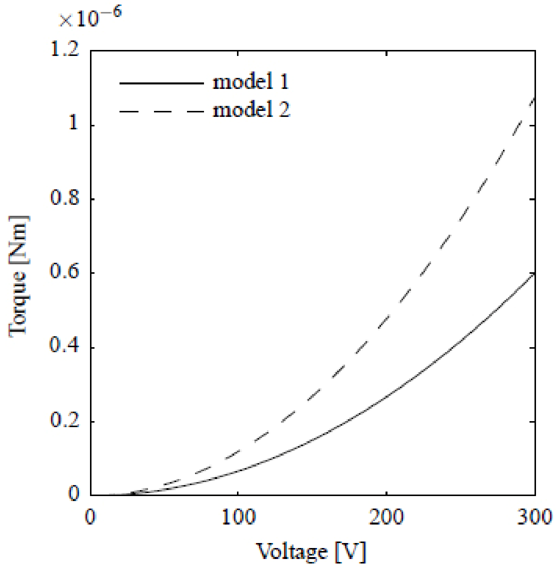

Figure 12 Applied voltage and resultant torque for the comb actuators.

4 MICRO-GRIPPER CONSTRUCTION METHOD

In the present section, the construction processes followed in order to obtain the compliant micro-mechanism are presented. The aim of this study is to obtain a device with suspended parts and other clamped zones. The device is a monolithic silicon based object composed of (see Figure 13):

- pads, used for the electrical polarization and clamped to an external platform with the electrical connections;
- comb-drives, used to carry out the claws, suspended and free to move on the plane of the device;
- claws, which are the device external parts and need both structural strength and flexibility.

All the moving parts are connected to the device suspended mainframe and consequently to the pads.
In order to obtain this structure a SOI (Silicon on Insulator) wafer has been used with device thickness of 40 μm, buried SiO_2 thickness of 3 μm and a handle thickness of 400 μm. This kind of substrate suites very well our purposes as it's possible to obtain suspended structures by etching, separately, the device and the handle silicon layers and, then, removing the oxide film. In this way the upper silicon parts are not in contact with the bottom parts.
The process sequence is based on DRIE (Deep Reactive Ion Etching), as the thickness of silicon to be etched is 40 μm for the device layer and 400 μm for the handle layer. Furthermore, vertical sidewalls are necessary for hinge bending.
The corresponding technological steps will be briefly resumed for the sake of completeness.

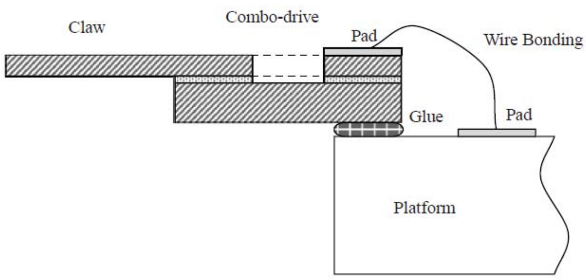

Figure 13 Device scheme.

With reference to Figures 14 and 15, the adopted process can be summarized as follows for both sides:

1. One layer of aluminum is deposited on the device layer surface by magnetron sputter deposition.
2. A photoresist layer is deposited on the aluminum layer by spin coating;
3. the mask is positioned between the wafer and the UV source in order to perform the exposure;
4. The mask geometry is transferred on the sample by photoresist developing;
5. Final geometry after photoresist developing;
6. the unprotected aluminum layer is etched by a solution of phosphoric acid (H3PO4,80%), nitric acid (HNO3,5%) and deionized water (DI,10%) and the geometry is transferred on aluminum;
7. Deep Reactive Ion Etching is applied on a SOI wafer;
8. Final 3D geometry after DRIE;
9. Etching of exposed silicon dioxide and separation of floating parts.

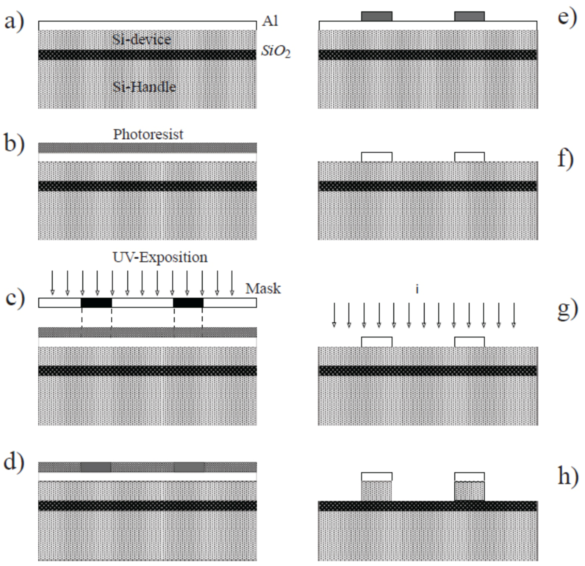

Figure 14 The process phases adopted for the Device Layer Etching.

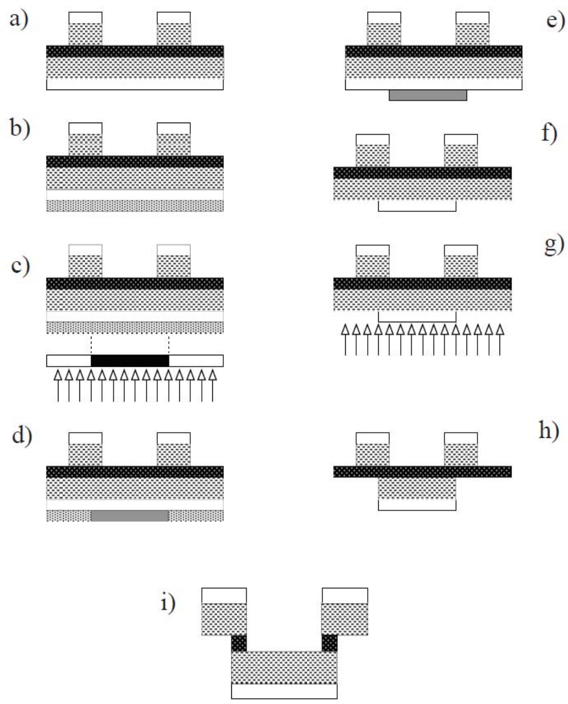

Figure 15 The process phases adopted for the Handle Layer Etching.

4.1 EXPERIMENTAL RESULTS OF THE DEVICE LAYER ETCHING PHASE

In this section the part of the construction process represented in Fig. 14, from a) to h), is briefly illustrated.

Fig. 16 shows an image of the top layer (device layer) obtained by means of a scanning electron microscope (SEM). The device geometry can be recognized. However, there are, in the Figure, also some separation lines, which can be recognized, that are extraneous to the device geometry, which have been etched in order to extract the sacrificial floating plates easily. Thanks to this image it is possible to observe that

- the device geometry is replicated with a acceptable accuracy;
- the curved lines are also well replicated, which is a critical issue for the proposed device;
- the aspect ratio is quite feasible for the application;
- comb drives are also constructed with a fair accuracy.

A preliminary test on the wafer has been performed by analyzing the morphology of the front layer after D-RIE process. Fig. 17 shows the actual feasibility of the comb drive construction process. The teeth have an acceptable shape and are separated by an acceptable gap. Fig. 18 presents a detailed view of the whole flexure hinge: the flexible curved beam, the adjacent links and even a view of the conjugate cylindrical surfaces. Finally, Fig. 19 shows the CSFH and the electrostatic comb drive of the device after the final step of the construction process: separation of the floating parts by etching of silicon dioxide.

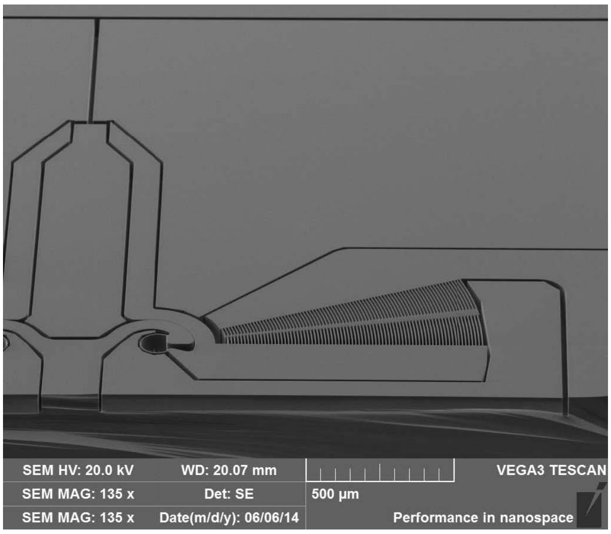

Figure 16 Etched wafer frontside: the sample is 30 degrees tilted and a section of it is visible in the lower portion of the image (FBK MNF Micro Nano Facility).

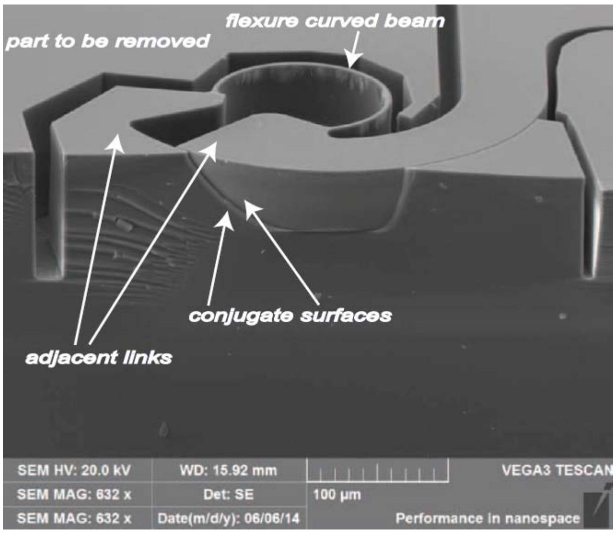

Figure 18 The flexure hinge and a pair of adjacent links before reaching the SiO2 layer (FBK MNF Micro Nano Facility).

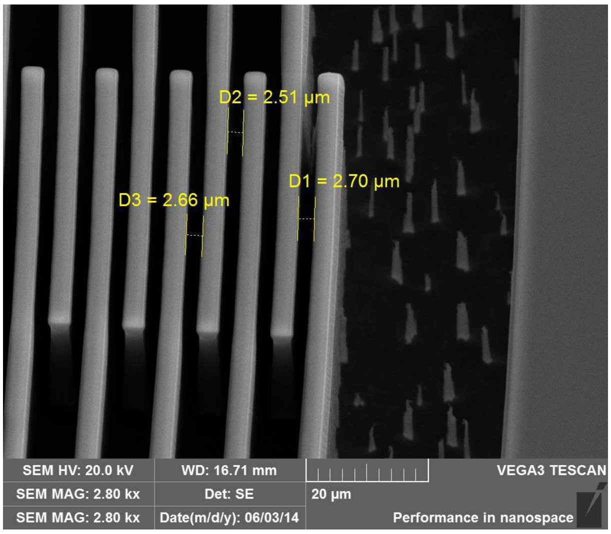

Figure 17 The teeth of the constructed comb drive (FBK MNF Micro Nano Facility).

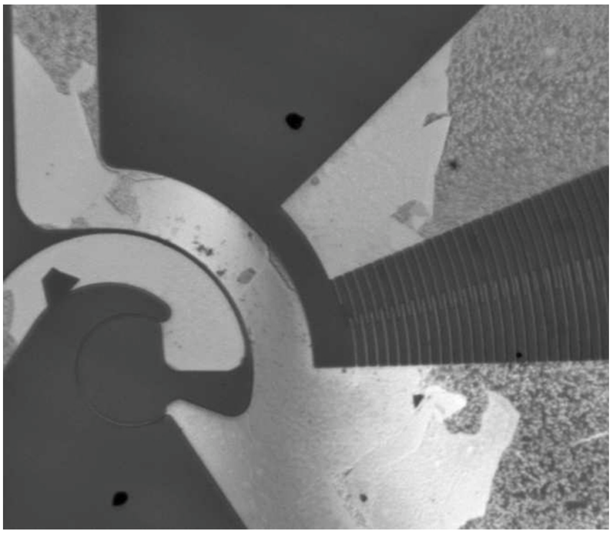

Figure 19 Device detail after the final step of the construction process: CSFH and electrostatic comb drive

5 CONCLUSION

This paper has shown how a new silicon micro gripper for micro manipulation can be designed, simulated and constructed. Although the overall size does not exceed 3×3 mm, with the smallest subpart thickness equal to about 3 µm, the experimental tests, after the top layer etching stage, showed a satisfying accuracy in geometry, also in curved lines replication. This characteristic is a crucial aspect for the proposed device because it gives an experimental proof that, generally speaking, silicon micro devices based on Conjugate Surfaces Flexure Hinges (CSFHs) can be constructed without problems.

REFERENCES

[1] Pisano A.P. Biomedical applications of MEMS: A look at grippers, cochlear implants, micro needles and microchemical assay devices. In *ASME DSC*, vol. 57-2, p.949, 1995.

[2] Havlik S. Modeling, analysis and optimal design of multi-component force/displacement sensors. In *Proc.on the First ECPD Int. Conf. on Advanced Robotics and Intelligent Automation*, pp. 283–289, Sept. 6-8, Athens, Greece,1995.

[3] Petrovic D., Popovic G., Chatzitheodoridis E., Del Medico O., Almansa A., Detter H. and Brenner W. Mechanical gripper system for handling and assembly

in MEMS. In *SPIE 2001*, vol. 4557, pp. 151–156, 2001.

[4] Seidemann V., Batefisch S. and Battgenbach S. Fabrication and investigation of in-plane compliant SU8 structures for MEMS and their application to micro valves and micro grippers. *Sensors and Actuators, A: Physical*, vol. 97-98, pp. 457–461, 2002.

[5] Enikov E. and Minkov L. Micro-assembly and packaging of MEMS using optically transparent electrostatic gripper. In *ASME MED*, vol. 15, pp. 511–518, 2004.

[6] Kang B. and Wen J. Design of compliant MEMS grippers for micro-assembly tasks. In *IEEE ICIRS*, pp. 760–765, 2006.

[7] Jeon C.S., Park J.S., Lee S.Y. and Moon C.W. Fabrication and characteristics of out-of-plane piezoelectric micro grippers using MEMS processes. *Thin Solid Films*, vol. 515, no. 12, pp. 4901–4904, 2007.

[8] Kim B., Park J.S., Moon C., Jeong G.M. and Ahn H.S. A precision robot system with modular actuators and MEMS micro gripper for micro system assembly. *Journal of Mechanical Science and Technology*, vol. 22, no. 1, pp. 70–76, 2008.

[9] Chen T., Chen L., Sun L., Wang J. and Li X. A sidewall piezoresistive force sensor used in a MEMS gripper. *Intelligent Robotics and Applications*, Springer Berlin Heidelberg, 2008.

[10] Chen T., Chen L., Liu B., Wang J. and Li X. Design of a four-arm structure MEMS gripper integrated with sidewall force sensor. In *NEMS 2009*, pp. 75–79, 2009.

[11] Chen T., Chen L., Sun L. and Li X. Design and fabrication of a four-arm-structure MEMS gripper. *IEEE Transactions on Industrial Electronics*, vol. 56, no. 4, pp. 996–1004, 2009.

[12] Chen D.S., Yin C.Y., Lai R.J. and Tsai J.C. A multiple degrees of freedom electrothermal actuator for a versatile MEMS gripper. In *IEEE MEMS 2009*, pp. 1035–1038, 2009.

[13] Mayyas M. and Stephanou H. Electrothermoelastic modeling of MEMS gripper. *Microsystem Technologies*, vol. 15, no. 4, pp. 637–646, 2009.

[14] Chen B., Zhang Y. and Sun Y. Novel MEMS grippers capable of both grasping and active release of micro objects. In *TRANSDUCERS 2009*, pp. 2389–2392, 2009.

[15] Vijayasai A., Sivakumar G., Mulsow M., Lacouture S., Holness A. and Dallas T. Haptic controlled three-axis MEMS gripper system. *Review of Scientific Instruments*, vol. 81, no. 10, 2010.

[16] Havlik S. Improving accuracy of compliant robotic (micro) devices. In *Proc. 19th International Workshop on Robotics in Alpe-Adria-Danube Region, RAAD 2010*, pp. 385–389, 2010.

[17] Hricko J., Havlik S. and Hart'ansky R. Optimization in designing compliant robotic micro-devices. In *Proc. 19th International Workshop on Robotics in Alpe-Adria-Danube Region*, pp. 397–402, 2010.

[18] Khazaai J., Qu H., Shillor M. and Smith L. An electrothermal MEMS gripper with large tip opening and holding force: Design and characterization. *Sensors and Transducers*, vol. 13, pp. 31–43, 2011.

[19] Khazaai J., Qu H., Shillor M., Smith L. and Cheok K. Design and fabrication of a metallic MEMS gripper using electro-thermal V-shape and modified U-shape actuators. In *NSTI-Nanotech 2011*, vol. 2, pp. 353–356, 2011.

[20] Kim B.S., Park J.S., Hun Kang B. and Moon C. Fabrication and property analysis of a MEMS microgripper for robotic micro-manipulation. *Robotics and Computer-Integrated Manufacturing*, vol. 28, no. 1, pp. 50–56, 2012.

[21] Abbasi A. and Ahmadian M. Force controlled manipulation of biological cells using a monolithic mems based nano-micro gripper. In *ASME IMECE*, vol. 2, pp.193–201, 2012.

[22] Piriyanont B. and Moheimani S. Design, modeling, and characterization of a MEMS micro-gripper with an integrated electrothermal force sensor. In *AIM 2013*, pp. 348–353, 2013.

[23] Piriyanont B., Moheimani S. and Bazaei A. Design and control of a MEMS micro-gripper with integrated electro-thermal force sensor. In *AUCC 2013*, pp. 479–484, 2013.

[24] Chen D.S., Yeh P.F., Chen Y.F., Tsai C.W., Yin C.Y., Lai R.J. and Tsai J.C. An electrothermal actuator with two degrees of freedom serving as the arm of a MEMS gripper. *IEEE Transactions on Industrial Electronics*, vol. 61, no. 10, pp. 5465–5471, 2014.

[25] Hao Y., Dong F., Zhang J. and Bao L. Study on microgripper based on MEMS mechanism assembly. *Zhongguo Jixie Gongcheng/China Mechanical Engineering*, vol. 25, no. 5, pp. 596–601, 2014.

[26] Belfiore N.P. and Pennestrì E. An atlas of linkage type robotic grippers. *Mechanism and Machine Theory*, vol. 32, no. 7, pp. 811–833, 1997.

[27] Belfiore N.P. Distributed databases for the development of mechanisms topology. *Mechanism and Machine Theory*, vol. 35, no. 12, pp. 1727–1744, 2000.

[28] Belfiore N.P. Brief note on the concept of planarity for kinematic chains. *Mechanism and Machine Theory*, vol. 35, no. 12, pp. 1745–1750, 2000.

[29] Belfiore N.P., Faralli M., Presta M., Moretti M., Ianniello F., Scaccia M. and Consorti L. On a test bench for studying lubrication in a spherical bearing:

Simulations and experimental validation. *Tribo Test*, vol. 12, no. 4, pp. 287–308, 2006.

[30] Belfiore N.P., Ianniello F., Natali S., Casadei F. and Stocchi D. The development of a feasible method for the tribological characterization of gear teeth surface treatments. *Tribology International*, vol. 39, no. 8, pp. 789–795, 2006.

[31] Belfiore N.P., Ianniello F., Stocchi D., Casadei F., Bazzoni D., Finzi A., Carrara S., González J., Llanos J.,Heikkila I., Peñalba F. and Gómez X. A hybrid approach to the development of a multilayer neural network for wear and fatigue prediction in metal forming. *Tribology International*, vol. 40, no. 10-12, pp. 1705–1717, 2007.

[32] Balucani M., Belfiore N., Crescenzi R. and Verotti M. The development of a MEMS/NEMS-based 3 D.o.F. compliant micro robot. *International Journal of Mechanics and Control*, vol. 12, no. 1, pp. 3–10, 2011.

[33] Balucani M., Belfiore N.P., Crescenzi R., Genua M. and Verotti M. Developing and modeling a plane 3 D.o.F. compliant micromanipulator by means of a dedicated mbs code. In *Technical Proceedings of the 2011 NSTI Nanotechnology Conference and Expo, NSTI-Nanotech 2011*, vol. 2, pp. 659–662. 2011.

[34] Belfiore N., Balucani M., Crescenzi R. and Verotti M. Performance analysis of compliant mems parallel robots through pseudo-rigid-body model synthesis. In *ASME 2012 11th Biennial Conference on Engineering Systems Design and Analysis, ESDA 2012*, vol. 3, pp. 329–334. 2012.

[35] Belfiore N., Verotti M. and Consorti L. Comparative analysis of isotropy indices in RR and RRP arms. *International Journal of Mechanics and Control*, vol. 11, no. 1, pp. 3–12, 2010.

[36] Belfiore N., Di Giamberardino P., Rudas I. and Verotti M. Isotropy in any RR planar dyad under active joint stiffness regulation. *International Journal of Mechanics and Control*, vol. 12, no. 1, pp. 75–81, 2011.

[37] Belfiore N.P., Verotti M., Di Giamberardino P. And Rudas I.J. Active joint stiffness regulation to achieve isotropic compliance in the Euclidean space. *Journal of Mechanisms and Robotics*, vol. 4, no. 4, pp. 041010 1–11, 2012.

[38] Belfiore N.P., EmamiMeibodi M., Verotti M., Crescenzi R. and adn P. Nenzi M.B. Kinetostatic optimization of a MEMS-based compliant 3 DOF plane parallel platform. In *IEEE 9th International Conference on Computational Cybernetics, ICCC*, Tihany, Hungary, 2013.

[39] Belfiore N.P., Verotti M., Crescenzi R. and Balucani M. Design, optimization and construction of MEMS - Based micro grippers for cell manipulation. In *IEEE International Conference on System Science and Engineering, ICSSE,* Budapest, Hungary, 2013.

[40] Belfiore N.P. Functional synthesis of a new class of micro electro-mechanical systems. *Advances in Soft Computing, Intelligent Robotics and Control*, vol. 8 of *Topics in Intelligent Engineering and Informatics*, pp. 81–93. Springer International Publishing, 2014.

[41] Pennestrì E. and Belfiore N.P. Modular third-order analysis of planar linkages with applications. In *American Society of Mechanical Engineers, Design Engineering Division (Publication) DE*, vol. 70-1, pp. 99– 103. 1994.

[42] Pennestrì E. and Belfiore N.P. On the numerical computation of generalized Burmester points. *Meccanica*, vol. 30, no. 2, pp. 147–153, 1995.

[43] Belfiore N.P., Prosperi G. and Crescenzi R. A simple application of conjugate profile theory to the development of a silicon micro tribometer. In *Proc. ASME 2014 12th Biennial Conf. on Eng. Systems Design and Analysis*. Copenhagen, Denmark, 2014.

[44] Verotti M., Crescenzi R., Balucani M. and Belfiore N.P. MEMS-Based Conjugate Surfaces Flexure Hinge. *Journal of Mechanical Design, Transactions of the ASME*, vol. 137, no. 1, pp. 012301–012301, 2015.

[45] Belfiore N.P., Scaccia M., Ianniello F. and Presta M. Selective compliance hinge World Intellectual Property Organization, WO/2009/034551, Int. Appl. No. PCT/IB2008/053697, Publ. Date March, 19th, 2009, US Patent Application No. 12/677975, 2011.

[46] Midha A., Norton T.W. and Howell L.L. On the nomenclature, classification and abstractions of compliant mechanisms. *Journal of Mechanical Design*, vol. 116, pp. 270–279, 1994.

[47] Howell L.L., Midha A. and Norton T.W. Evaluation of equivalent spring stiffness for use in a pseudo rigid-body model of large-deflection compliant mechanisms. *Journal of Mechanical Design, Trans. ASME*, vol. 118, pp. 126–131, 1996.

[48] Howell L.L. *Compliant Mechanisms*. John Wiley & Sons, 2001.

[49] Belfiore N.P. and Simeone P. Inverse kinetostatic analysis of compliant four-bar linkages. *Mechanism and Machine Theory*, vol. 69, pp. 350 – 372, 2013.

[50] Chang H., Zhao H., Ye F., Yuan G., Xie J., KraftM. And Yuan W. A rotary comb-actuated microgripper with a large displacement range. *Microsystem Technologies*, vol. 20, no. 1, pp. 119–126, 2014.

[51] Andrew Yeh J., Huang J.Y., Chen C.N. and Hui C.Y. Design of an electrostatic rotary comb actuator. *Journal of Micro/Nanolithography, MEMS, and MOEMS*, vol. 5, no. 2, pp. 023008–023008–13, 2006.